Gel transitions in colloidal suspensions

1999 J. Phys.: Condens. Matter 11 10171

(http://iopscience.iop.org/0953-8984/11/50/310)

J. Phys.: Condens. Matter **11** (1999) 10171–10182. Printed in the UK PII: S0953-8984(99)06365-1

Gel transitions in colloidal suspensions

J Bergenholtz†§ and M Fuchs‡

† Department of Physical Chemistry, Göteborg University, 412 96 Göteborg, Sweden
‡ Physik-Department, Technische Universität München, 85747 Garching, Germany

Received 21 July 1999

Abstract. The idealized mode-coupling theory (MCT) is applied to colloidal systems interacting via short-range attractive interactions of Yukawa form. At low temperatures, MCT predicts a slowing down of the local dynamics and ergodicity-breaking transitions. The non-ergodicity transitions share many features with the colloidal gel transition, and are proposed to be the source of gelation in colloidal systems. Previous calculations of the phase diagram are complemented with additional data for shorter ranges of the attractive interaction, showing that the path of the non-ergodicity transition line is then unimpeded by the gas–liquid critical curve at low temperatures. Particular attention is given to the critical non-ergodicity parameters; this is motivated by recent experimental measurements. An asymptotic model is developed, valid for dilute systems of spheres interacting via strong short-range attractions, and is shown to capture all aspects of the low-temperature MCT non-ergodicity transitions.

1. Introduction

Colloidal particles interacting with strong attractions aggregate to form interesting structures. One such case is that of gel formation, which occurs when the interparticle attraction is strong and of short range relative to the particle size. Gelation of colloidal systems appears to be a common, if not universal, phenomenon, as it has been observed experimentally in numerous quite different colloid-like systems. Notable examples of gel-forming systems include colloid–polymer mixtures [1–7], in which the polymer is non-adsorbing and of low molecular weight, and suspensions of sterically stabilized particles in marginal solvents [8–13]. Emulsions [14], emulsion–polymer mixtures [15], colloid–surfactant mixtures [16, 17], and globular protein systems [18–21] are other examples of colloidal systems that exhibit gel formation.

The phase diagrams of the colloid–polymer mixtures have been examined in detail, revealing that they are of the gas–solid type without a triple point and without a liquid phase when the attraction is short ranged. The disappearance of the liquid phase is a well-documented effect [22–28], which is caused by the restricted range of the attraction. This situation is rather unique to colloidal systems in that most molecular attractions are of comparable range to the molecular dimension, precluding such phase behaviour.

Whereas the equilibrium phase behaviour of these systems is well understood, a fundamental understanding of the gel transition has been more difficult to achieve. Colloidal gels are characterized by ramified structures with particles located predominantly in clusters [6, 7]. It is thus natural to attempt to describe this phenomenon with percolation theories. This may seem especially appropriate in that density fluctuations are very slow near the gel transition, and particle clusters behave as nearly static objects [11]. However, rather poor

§ Author to whom any correspondence should be addressed.

0953-8984/99/5010171+12$30.00

agreement results when the percolation transition is compared to the experimental results for the gel transition line in the phase diagram, showing that the density dependence of the percolation transition is too strong [10, 11].

Another suggestion has been put forward in which the gel transition is attributed to dynamic percolation within a gas–liquid binodal which is metastable with respect to gas–solid coexistence [7]. Such metastable binodals have been observed also in solutions of globular proteins. However, gel (or precipitate) formation appears to occur in these systems also in regions of the phase diagram outside the metastable binodal [20], suggesting that the gel transition is not just triggered by an instability towards local density fluctuations. The same seems to hold for sterically stabilized suspensions as well, which exhibit a gel transition at supercritical temperatures [11]. Nevertheless, the same suspensions do form gels also under metastable conditions [11], as do colloid–polymer mixtures [3–5, 7, 29], prompting careful studies of any connection between the gel transition and metastability [7, 29].

We have recently suggested an explanation for the gel transition in reference [30], referred to henceforth as I. In this scenario, colloidal systems form gels as a result of an arrested structural relaxation due to the self-trapping mechanism called the cage effect [31–34], which is the same effect as is often thought to be responsible for the liquid–glass transition. The idealized mode-coupling theory (MCT), formulated with the aim of describing the cage effect in dense liquids, was seen to contain a bifurcation separating ergodic from non-ergodic motion also for systems of particles interacting via strong short-range attractive interactions. In I we attributed the non-ergodic states to gel formation; hence, our suggestion is that the gel transition can be described within the same theoretical framework as the liquid–glass transition.

Many of the qualitative aspects of the gel transition were found to be reproduced by the MCT calculations for the hard-core attractive Yukawa (HCAY) system. The calculated phase diagrams were found to exhibit gel transition lines that connect smoothly with the hard-sphere glass transition at high temperature and extend to the critical and subcritical regions at low temperature along paths that depend critically on the range of the attraction. The phase diagram obtained by Verduin and Dhont [11] is qualitatively reproduced by the MCT when the attraction is of intermediate range such that the gel transition meets the critical point. For shorter-range attractions the gel transition passes above the critical point, suggesting that structural arrest occurs instead of gas–liquid phase separation, which appears to agree with some measurements on sterically stabilized particle systems [9, 10, 12, 13].

A finite zero-frequency shear modulus is predicted by MCT, in agreement with many measurements on colloidal gels [7, 9, 10, 13]; this is expected to be intimately connected with a finite yield stress observed in other measurements [35]. At present, the theory cannot account for the density dependence of the modulus, indicating that the mesoscopic structure of the gels is important and is not captured correctly. In addition, the theory alone cannot explain the growth of the small-angle peak of the static structure factor nor the fractal scaling of its peak position observed on quenching of many suspensions [7]. It does, however, provide an explanation for why the growth of the small-angle peak slows down and finally arrests following deeper quenches. Very differently from earlier approaches, which attributed the ultimate gel arrest to a global jamming or percolation transition, our microscopic theory predicts the structural arrest to be driven by anomalies of and a slowing down of the local dynamics.

The purpose of this article is to provide a more detailed account of the results of the model study in I. In particular, the non-ergodicity parameters (cf. section 2.1) for several attraction ranges will be given; this is motivated by the recent measurements on colloid–polymer systems by Poon and co-workers [36]. In addition, a detailed description is given of the asymptotic model developed in I. This model captures the relevant features associated with our suggested scenario for gel formation. A discussion of the relevance of these results is also included.

2. Theory of colloidal gelation

2.1. Mode-coupling theory

The idealized mode-coupling theory (MCT) assumes that the dominant mechanism for structural relaxation in dense liquids is the cage effect. At short times, particles are trapped in the surrounding cage of neighbouring particles. At longer times, particle escape from the cage leads to structural relaxation to equilibrium. For sufficiently strong interactions, a bifurcation occurs in the governing equations—interpreted as the permanent entrapment of particles within their cages—causing the intermediate scattering function $F_q(t)$ to acquire a non-zero long-time limit known as the non-ergodicity parameter, glass form factor, or Debye–Waller factor $f_q = F_q(t \to \infty)/S_q$, where S_q is the structure factor and q is the modulus of the wavevector. The transition from a vanishing to a finite long-time limit of $F_q(t)$ is discontinuous and defines the liquid–glass transition within MCT. It is not a conventional thermodynamic phase transition, but rather an entirely dynamic transition, interpreted generally as an ergodic–non-ergodic transition. This simplified scenario captures many aspects of the liquid–glass transition in molecular liquids [31, 33] as well as hard-sphere suspensions [32, 33, 37–40].

The governing MCT equation for the time evolution of the intermediate scattering function reduces in the long-time limit to

$$\begin{aligned} \frac{f_q}{1-f_q} &= \frac{\rho}{2(2\pi)^3 q^2} \int \mathrm{d}\boldsymbol{k}\; V(\boldsymbol{q},\boldsymbol{k})^2 S_q S_k S_{|\boldsymbol{q}-\boldsymbol{k}|} f_k f_{|\boldsymbol{q}-\boldsymbol{k}|} \\ V(\boldsymbol{q},\boldsymbol{k}) &= \hat{\boldsymbol{q}}\cdot(\boldsymbol{q}-\boldsymbol{k}) c_{|\boldsymbol{q}-\boldsymbol{k}|} - \hat{\boldsymbol{q}}\cdot\boldsymbol{k} c_k \end{aligned} \tag{1}$$

where ρ is the number density and $c_q = (1 - S_q^{-1})/\rho$, which appears in the vertex function $V(\boldsymbol{q}, \boldsymbol{k})$, is the Fourier-transformed direct correlation function. Consideration of the single-particle motion leads to another set of equations for the incoherent non-ergodicity parameter f_q^s (also known as the Lamb–Mössbauer factor):

$$\begin{aligned} \frac{f_q^s}{1-f_q^s} &= \frac{\rho}{(2\pi)^3 q^2} \int \mathrm{d}\boldsymbol{k}\; V^s(\boldsymbol{q},\boldsymbol{k})^2 S_k f_k f^s_{|\boldsymbol{q}-\boldsymbol{k}|} \\ V^s(\boldsymbol{q},\boldsymbol{k}) &= \hat{\boldsymbol{q}}\cdot\boldsymbol{k} c_k \end{aligned} \tag{2}$$

where $f_q^s = F_q^s(t \to \infty)$, with the self-intermediate scattering function $F_q^s(t)$.

For a given S_q, equations (1) and (2) are closed equations for f_q and f_q^s. They are solved numerically by iteration starting from the initial iterate $f_q = f_q^s = 1$. With this starting point the iteration converges monotonically to the correct solution for the non-ergodicity parameters, given by the largest solution to the equations [41]. The wavevector integrations are performed efficiently using Simpson's rule on a uniformly discretized grid: $q = i\,\Delta q$, $i = 0, \ldots, N$. The critical glass transition boundary is identified by bracketing of the given input conditions, such as temperature and density, which delineates regions where f_q is zero and finite; regions of the phase diagram which result in finite non-ergodicity parameters are identified as glass states. Most calculations were done with the parameters $\Delta q = 0.3\sigma^{-1}$ and $N = 800$.

2.2. Model system

The hard-core attractive Yukawa (HCAY) interaction potential captures both short-range excluded-volume interactions and variable-range attractive particle interactions. It is given by

$$u(r)/k_B T = \begin{cases} \infty & 0 < r < \sigma \\ -\dfrac{K}{r/\sigma}\mathrm{e}^{-b(r/\sigma-1)} & \sigma < r \end{cases} \tag{3}$$

where the dimensionless parameter K regulates the depth of the attractive well and the reduced screening parameter b sets the range of the attraction.

The equilibrium phase diagrams for a number of attraction ranges have been obtained by computer simulations [27], showing that the liquid phase does indeed disappear upon restricting the range of the attraction. Because the HCAY static structure factor is known semi-analytically from the mean-spherical approximation (MSA) [42–44], it is convenient to base our study on this case. The penalty is that the resulting predictions are limited not only by the approximations made in the MCT, but also those made in the MSA. Therefore, the results should be viewed as qualitative rather than quantitative.

2.3. The asymptotic model

In the following we describe an asymptotic model, originally developed in I, that captures the relevant features of the suggested gelation mechanism. At low densities ($\phi = \pi\rho\sigma^3/6 \to 0$) the Ornstein–Zernike direct correlation function becomes independent of density. Specifying this in the MSA of the HCAY fluid, we obtain $c_q \to Kb(\sigma/b)^3\tilde{c}(q, \sigma, b)$, where

$$\tilde{c}(q, \sigma, b) = (b/\sigma)^2 \int_{r>\sigma} \mathrm{d}\boldsymbol{r}\ \mathrm{e}^{-b(r/\sigma-1)}\mathrm{e}^{\mathrm{i}\boldsymbol{q}\cdot\boldsymbol{r}}/r$$

in which we have neglected the contribution from the hard core, which is independent of K and b at low densities. In the limit of strong attractive interactions at low densities, the following scaling simplifies the MCT equations:

$$\phi \to 0 \qquad \text{and} \qquad K \to \infty \qquad \text{so } \Gamma = \frac{K^2\phi}{b} = \text{constant.} \tag{4}$$

In addition, $S_q \to 1$ in this limit and the MCT equations (1) and (2) simplify considerably such that the non-ergodicity transitions occur at $\Gamma = \Gamma_c(b)$, leading to the asymptotic prediction $K_c \propto 1/\sqrt{\phi}$.

For short-range attractive interactions, in the limit $b \to \infty$, a further simplification arises because the MCT vertex functions become linear functions of Γ only, if we introduce the rescaled wavevectors $\tilde{q} = q\sigma/b$. Equation (1) simplifies to

$$\frac{\tilde{f}_{\tilde{q}}}{1-\tilde{f}_{\tilde{q}}} = \frac{\Gamma}{\tilde{q}^2}\int \mathrm{d}\tilde{\boldsymbol{k}}\ \tilde{V}(\tilde{\boldsymbol{q}}, \tilde{\boldsymbol{k}})^2 \tilde{f}_{\tilde{k}}\tilde{f}_{|\tilde{\boldsymbol{q}}-\tilde{\boldsymbol{k}}|} \tag{5}$$

with the dominant contribution to the rescaled vertex function given as

$$\begin{aligned}\tilde{V}(\tilde{\boldsymbol{q}}, \tilde{\boldsymbol{k}})^2 &= \tilde{V}^s(\tilde{\boldsymbol{q}}, \tilde{\boldsymbol{q}}-\tilde{\boldsymbol{k}})^2 + \tilde{V}^s(\tilde{\boldsymbol{q}}, \tilde{\boldsymbol{k}})^2 \\ \tilde{V}^s(\tilde{\boldsymbol{q}}, \tilde{\boldsymbol{k}})^2 &= \frac{3}{\pi^2}\frac{(\tilde{\boldsymbol{q}}\cdot\tilde{\boldsymbol{k}})^2}{\tilde{q}^2\tilde{k}^2(1+\tilde{k}^2)}\end{aligned} \tag{6}$$

where the non-ergodicity parameters depend only on the rescaled wavevectors $f_q \to \tilde{f}_{\tilde{q}}$. The same set of equations is found to govern the incoherent non-ergodicity parameters $\tilde{f}^s_{\tilde{q}}$. Note that in this limit single-particle and collective non-ergodicity factors are identical and exhibit the small-wavevector expansion $\tilde{f}_{\tilde{q}} = 1 - \tilde{q}^2(r_s b/\sigma)^2$, where r_s is the localization length, or root mean square displacement, in the glass.

In this limit the coupling constant Γ assumes a unique value at the transitions, which is found from solving equations (5) and (6) numerically, resulting in $\Gamma_c \approx 3.02$ for $b \to \infty$. We emphasize that these asymptotic forms are valid for the HCAY systems using the MSA in the prescribed limits.

3. Results

3.1. Phase diagrams

Using the MSA static structure factor [42–44] as input, the MCT was solved for several screening parameters: $b = 7.5$, 20, 30, and 40. The progression of the glass transition can be traced from the (Percus–Yevick) hard-sphere limit, corresponding to $K = 0$, to lower temperatures in terms of the reduced temperature K^{-1}. In I we showed the phase diagrams for $b = 7.5$, 20, and 30. This work adds an additional phase diagram for $b = 40$.

As shown in I, at low temperatures (large values of K) the glass transition is traced along different paths in the phase diagrams depending on the value of the screening parameter, i.e. the range of the attractive interaction. In all cases they bend towards lower densities when the temperature is decreased sufficiently. The transition lines for intermediate-range attractions ($b = 7.5$ and 20) reach subcritical temperatures on the liquid side of the spinodal. For shorter ranges of the attraction ($b = 30$) the non-ergodicity transition line lies entirely within the fluid phase above the two-phase region, and extends to subcritical temperatures at low densities on the vapour side of the spinodal. This is shown in detail in figure 1, in which the results for $b = 30$ and 40 are given. As seen, decreasing the attraction range further to $b = 40$ causes the non-ergodicity transition line to move away from the spinodal curve. In contrast to the case for the MSA phase diagrams studied in I, the $b = 40$ transition line is located sufficiently far away from the spinodal curve to remove the additional non-ergodicity transition line that appears in the MSA phase diagrams with lower b. This type of transition is discussed in the appendix of

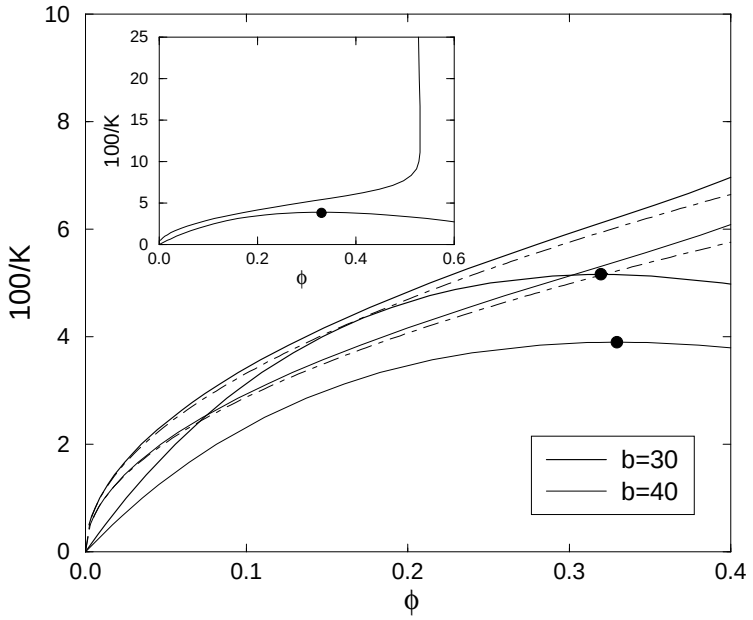

Figure 1. Enhancement of the low-density and low-temperature region of the HCAY diagrams for $b = 30$ and 40. The MSA spinodal curves are shown with the critical points denoted by •, together with the corresponding MCT non-ergodicity transition lines as labelled. The chain curves correspond to the asymptotic prediction in equation (4) and $b \to \infty$ with $\Gamma_c(b \to \infty) = 3.02$. The inset shows the phase diagram for $b = 40$ for the same density and temperature ranges as in figure 2 of I.

I. Also shown in figure 1 are the spinodal curves, defined by the condition $S_q \to \infty$ for $q \to 0$. In the present context they are shown as an indication of where gas–liquid phase separation is likely to occur, provided that a liquid phase is present.

As pointed out in I, the MCT non-ergodicity transition lines resemble the gel transition lines determined experimentally. Most notably, the diagram with $b = 20$ (see I), which displays a near meeting of the non-ergodicity transition and the critical point, bears a strong resemblance to the phase diagram determined by Verduin and Dhont [11] in their measurements of sterically stabilized silica suspensions. Other measurements on sterically stabilized suspensions found a gel transition line with no apparent evidence of phase separation, which can be expected, according to the MCT, for attractions of very short range, such as for $b = 30$ or 40 in figure 1.

One important aspect of the MCT non-ergodicity transitions is that they are not induced by long-range structural correlations associated with critical fluctuations. This is demonstrated by the asymptotic model which is valid in the limit in equation (4) and $b \to \infty$ for which $S_q \approx 1$. The predictions of the model are shown in figure 1 as chain curves. There is quantitative agreement at low densities and the model predictions reproduce the results of the full calculation for the non-ergodicity transitions qualitatively at moderately high densities. The agreement with the asymptotic model demonstrates that the $q \to 0$ limit of S_q is decoupled from the structural arrest at low densities and temperatures. This conclusion is of particular importance as not all relevant mode couplings expected for systems near the critical point [45] are included in this version of MCT.

3.2. Non-ergodicity parameters

Dynamic light scattering measurements of the non-ergodicity parameters led, *inter alia*, to the identification of the glass transition for the colloidal hard-sphere system [37–40]. As MCT predicts very different behaviour for these when strong short-range attractions are present [30], it can be expected that such measurements will provide a similarly decisive test of the MCT of gelation. For that reason we focus here on the behaviour of the non-ergodicity parameters as functions of density and temperature.

When the attraction is of moderately short range, such as for $b = 7.5$, figure 2 shows that the coherent non-ergodicity parameters deviate little from the hard-sphere f_q as the temperature is lowered, with the exception of an increasing $q \to 0$ value. Note that the f_q shown in figure 2 and later figures are the critical non-ergodicity parameters, which appear along the MCT transition lines shown in figure 2 of I and figure 1 of this work. The increase of the $q \to 0$ value results in this case mainly from the increased contribution of long-range correlations, which derive from the increase of the $q \to 0$ limit of S_q upon approaching the liquid side of the spinodal curve. Shown also in figure 2 is the prediction from the asymptotic model based on equation (4) and $b \to \infty$, which does not capture the behaviour of f_q at the lowest temperatures. This should be expected, as the attraction is not particularly short ranged.

Decreasing the range of the attractive interaction to $b = 20$, which causes the non-ergodicity transition line to move closer to the critical point (see figure 2 of I), leads now to form factors that deviate more from hard-sphere behaviour at low temperatures. Compared to the case for $b = 7.5$, this shorter-range attraction causes coupling among more wavevector modes, leading to an increase in the width of f_q as the temperature is decreased. This effect is produced by the increased width of the static structure factor, caused by strong short-range correlations due to the attraction. As in the case of $b = 7.5$, the $q \to 0$ limit of f_q for $b = 20$ increases when the temperature is decreased. Now, however, the asymptotic model yields a reasonably accurate prediction for f_q at the lowest temperatures, which can be expected from the rather close agreement between the asymptotic model and the full calculation of the

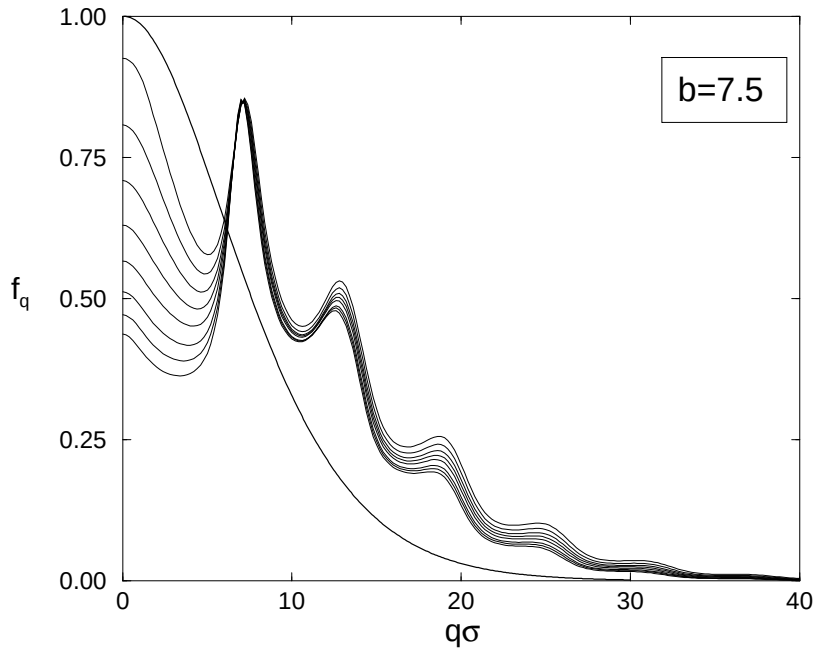

Figure 2. HCAY critical coherent non-ergodicity parameters f_q for $b = 7.5$ along the critical boundary as functions of normalized wavevector $q\sigma$ and Yukawa prefactor K. Note that the volume fraction varies according to the $b = 7.5$ non-ergodicity transition line in figure 2 of I. The K-values, incremented by 1, run from bottom to top from 0 to 7. The curve shown in bold gives the asymptotic prediction resulting from equation (4) and $b \to \infty$.

transition line for $b = 20$.

When the range of the attraction is decreased further by changing the HCAY screening parameter to $b = 30$, the path of the non-ergodicity transition is unimpeded by the gas–liquid critical curve (see figure 1); it extends to subcritical temperatures on the low-density, vapour side of the spinodal curve. The form factors along the transition, shown in figure 4, are qualitatively similar to those corresponding to $b = 20$, except that the width of f_q is further increased due to the stronger short-range correlations. The agreement with the asymptotic model is improved at the lower temperatures where the oscillations in f_q are now somewhat suppressed. The improved agreement should be expected because the asymptotic model is based in part on the limit $\phi \to 0$, which can be fulfilled by this system as the non-ergodicity transition line lies entirely in the (very probably metastable) single-phase fluid regime.

The dynamics of the gel transitions can be expected to be anomalously stretched over many orders in time and to exhibit a rapid slowing down upon approaching the non-ergodicity transition lines. As discussed in detail in reviews of the MCT [31, 33], this and a number of other qualitative aspects can be understood from the factorization property and asymptotic expansions, which describe the sensitive variation of the cage dynamics close to the transition. One finds: $F_q(t)/S_q = f_q^c + h_q G^\lambda(t)$. As the so-called β-correlator, $G^\lambda(t)$, also exhibits numerous universal features depending on one material parameter only, the exponent parameter λ, this expression provides for crucial experimental tests of MCT transition scenarios, such as those performed for hard-sphere colloids [38–40]. We find $\lambda = 0.89$ [30], predicting a very anomalous stretching and rapid increase of the longest relaxation time [31,33]. Figure 5 shows the two wavevector-dependent amplitudes, which describe the gel structure (f_q^c, also included

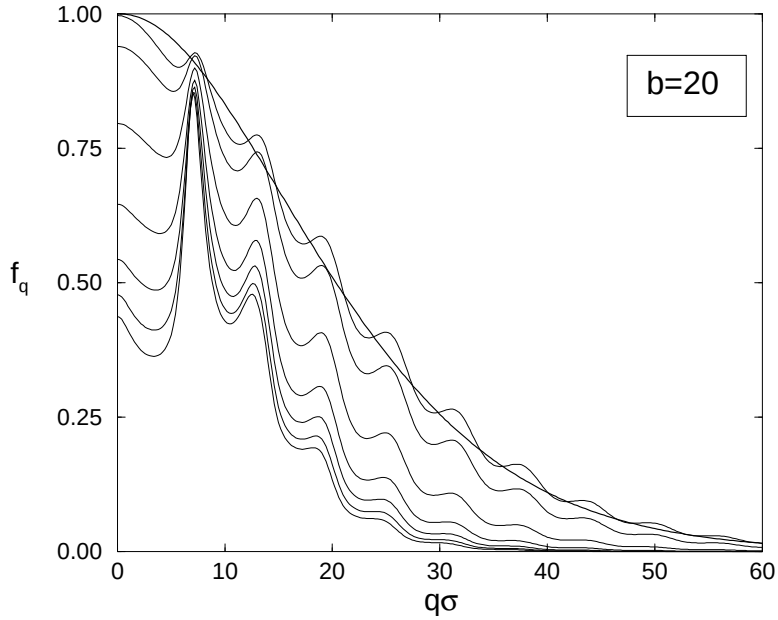

Figure 3. HCAY critical coherent non-ergodicity parameters f_q for $b = 20$ as in figure 2. The K-values, incremented by 2, run from bottom to top from 0 to 12. The asymptotic prediction from equation (4) is shown as the bold curve.

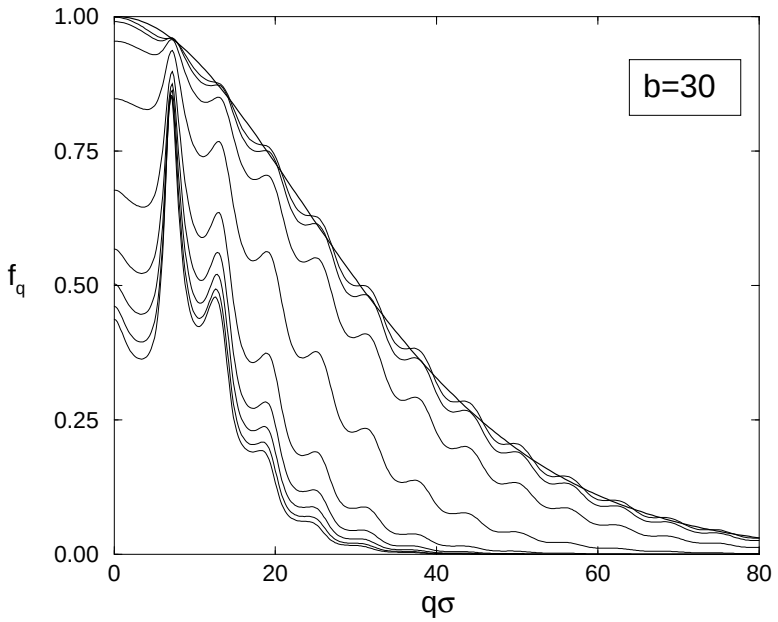

Figure 4. HCAY critical coherent non-ergodicity parameters f_q for $b = 30$ as in figure 2. The K-values, incremented by 2, run from bottom to top from 0 to 16. The asymptotic prediction from equation (4) is shown as the bold curve.

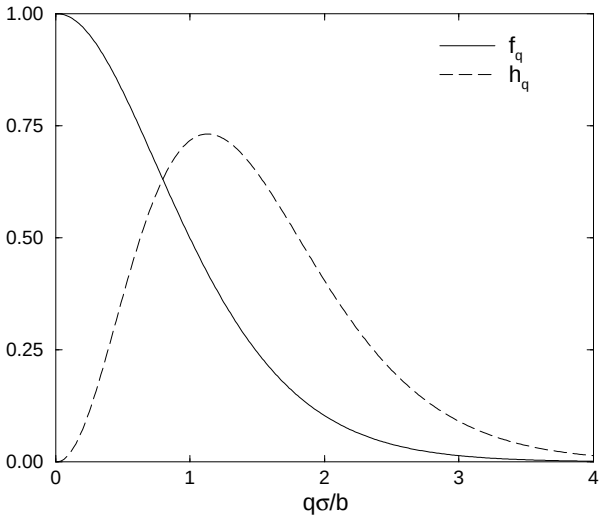

Figure 5. The critical coherent non-ergodicity parameter f_q and amplitude factor h_q as functions of the scaled wavevector for the asymptotic model in equations (4)–(6) and $b \to \infty$.

in figures 2–4) and localized cage dynamics (h_q). The amplitude factor h_q, which describes the spatial extent of that dynamical process which arrests at the gel transition, is found to be peaked at rather large wavevectors, stressing that the local motion of the colloids is suppressed at the gel transitions.

4. Discussion and conclusions

Structural arrest as described by the idealized MCT is found to be a plausible explanation for colloidal gelation. The underlying cause of gelation in this scenario is a breaking of ergodicity caused by strong short-range attractions in dilute systems. An ergodic–non-ergodic transition is characteristic also for the glass transition within the framework of MCT. The low-temperature gel transitions are accompanied by the cessation of hydrodynamic diffusion and the appearance of rather large finite elastic moduli due to the particles being tightly localized in ramified clusters (for more details see I).

At relatively high temperatures, corresponding to weak attractions among the suspended particles, the cage surrounding a typical particle is distorted by dimerization [46] (see also [30]). The cage must be reinforced by increasing the critical colloid density before structural arrest ensues, which leads to a glass transition line that moves initially towards higher density with decreasing temperature. This trend appears to require hard-core repulsions and becomes more pronounced when the range of the attractive interaction decreases. It has been observed in the adhesive hard-sphere system [30, 46] and the Yukawa systems investigated in I and this study. For the colloid–polymer mixtures, recrystallization of glassy samples has been reported upon introducing a small concentration of low-molecular-weight non-adsorbing polymer [4]. We attribute this effect to the glass transition line possessing an initial slope in accordance with the MCT predictions, i.e. in the direction of higher density with decreasing temperature.

Stronger short-range attractions cause particle aggregation, leading in effect to an increase of the density in the local environment of a typical particle. According to MCT, aggregation can lead to structural arrest of the long-time dynamics despite the bulk density being much

lower than the hard-sphere glass transition density. As shown in I and figure 1, the precise path of the non-ergodicity transition line in the phase diagram depends now critically on the range of the attraction; this is reminiscent of the dependence of the freezing line on the range of the attraction [22–28].

The low-density non-ergodicity transitions, which appear only for sufficiently short ranges of the attraction, are not only caused by the excluded-volume effect which dominates at higher densities, but are additionally affected by the low- and high-q behaviour of the static structure factor. The asymptotic model demonstrates, however, that the short-range (high-q) correlations become increasingly important as the range of attraction is decreased, such that they are the dominant cause of the structural arrest at low densities. This observation indicates that the non-ergodicity transitions are unaffected by long-range correlations and the presence of the critical point. Thus the fact that the MCT transitions occur in close proximity to the spinodal curve for a significant range of b is merely coincidental. The results shown in figure 1 are in accord with this conclusion; the non-ergodicity transition line for $b = 40$ is seen to be located further away from the critical curve than for $b = 30$.

Nevertheless, several studies, particularly the extensive ones of the colloid–polymer mixtures, reveal what appears to be an intimate connection between the gel transition and the metastable gas–liquid binodal. It is possible that the gel transition changes character once it crosses the metastable binodal into the metastable and unstable regions. This is not in disagreement with our description of the arrest of the local dynamics, but indicates that the large-distance dynamics can be more complicated. Unfortunately we are as yet unable to make any predictions for inside the unstable region with the present MCT, because an appropriate S_q is not available and the theory assumes closeness to equilibrium [33].

Krall and Weitz [47] have studied low-density gels experimentally at small wavevectors, though still larger than the wavevectors characterizing the small-angle scattering peak. The low-density gels are associated with finite non-ergodicity parameters, supporting the MCT gelation mechanism. However, Krall and Weitz measure relatively small values for the non-ergodicity parameters, whereas the full MCT solutions, as well as the asymptotic model described in section 2.3, predict large values for f_q at small wavevectors. Such large values are observed experimentally also, but only at somewhat higher densities. We are attempting currently to locate a low-density region in the MSA phase diagrams with this type of dynamics.

Experimental measurements of the dynamics of gels at higher densities have been conducted. Sterically stabilized suspensions [11] and colloid–polymer mixtures with low-molecular-weight polymer [36] show that these gels are associated also with finite non-ergodicity parameters, further supporting the present model calculations. Moreover, the measured f_q assume values not too much below unity both at low q [11] and at values near the q corresponding to the principal peak of S_q [36].

Poon and co-workers [29] have made detailed studies of the low-density and low-temperature region of the colloid–polymer phase diagram for low-molecular-weight polymers. They identified a variety of different dynamics which can be reconciled with the MCT calculations provided that their system belongs to the HCAY diagram with $b \approx 20$. For such a situation the gel transition meets the spinodal on the liquid side, without interfering with the critical behaviour along the vapour side. Conjecturing that the gel transition can exist in the unstable region as found experimentally by Verduin and Dhont [11], we obtain a phase diagram qualitatively similar to that determined by Poon *et al* [29]. We expect that quenching of a suspension at low to moderately low density results initially in normal phase-separation dynamics, characterized by either spinodal decomposition or nucleation and growth. This process proceeds until the denser domains reach the critical density for gelation, subsequently arresting the structure, which would be consistent also with the measurements in reference [11].

Thus we anticipate that the so-called transient gelation region, discovered by Poon *et al* [29] for colloid–polymer systems with short polymers, corresponds to a non-ergodicity transition in the unstable region of the phase diagram.

The asymptotic model of section 2.3 provides additional support for this interpretation. First, arrest of long-range structures is caused by an arrest of the local dynamics. In contrast to the case for percolation approaches for the gel arrest, the local density fluctuations also exhibit slowing down and dynamical anomalies. Second, the tight localization of the particles provides a rationale for using concepts like bond formation and sticking probabilities, even though the particles obey diffusive equations of motion. Third, the approach to unity of the collective non-ergodicity or Debye–Waller factors for small wavevectors, $f(q) \to 1$ for $q \to 0$, indicates that the particles are bound to infinite clusters in this limit. Momentum conservation, or Newton's law of action and reaction, otherwise would require $f(q \to 0) < 1$, as found for glasses.

In summary, gelation in colloidal systems is attributed to a breaking of ergodicity, captured qualitatively by the MCT applied to the HCAY system. The calculated phase diagrams show many similarities to those determined experimentally for colloid–polymer mixtures and sterically stabilized suspensions. Decreasing the range of the attractive interaction sufficiently causes the gel transition to move further into the single-phase region. The gross features of the MCT non-ergodicity parameters at low temperatures are seen to be in accord with the few existing measurements, supporting the proposed gelation mechanism.

Acknowledgments

Financial support by the Deutsche Forschungsgemeinschaft (DFG) (Grant No Fu309/2-1) is gratefully acknowledged.

References

[1] Patel P D and Russel W B 1989 *J. Colloid Interface Sci.* **131** 192
[2] Emmett S and Vincent B 1990 *Phase Transitions* **21** 197
[3] Poon W C K, Selfe J S, Robertson M B, Ilett S M, Pirie A D and Pusey P N 1993 *J. Physique* II **3** 1075
[4] Ilett S M, Orrock A, Poon W C K and Pusey P N 1995 *Phys. Rev.* E **51** 1344
[5] Poon W C K, Pirie A D and Pusey P N 1995 *Faraday Discuss.* **101** 65
[6] Verhaegh N A M, Asnaghi D, Lekkerkerker H N W, Giglio M and Cipelletti L 1997 *Physica* A **242** 104
[7] Poon W C K and Haw M D 1997 *Adv. Colloid Interface Sci.* **73** 71
[8] Jansen J W, de Kruif C G and Vrij A 1986 *J. Colloid Interface Sci.* **114** 481
[9] Chen M and Russel W B 1991 *J. Colloid Interface Sci.* **141** 564
[10] Grant M C and Russel W B 1993 *Phys. Rev.* E **47** 2606
[11] Verduin H and Dhont J K G 1995 *J. Colloid Interface Sci.* **172** 425
[12] Rueb C J and Zukoski C F 1997 *J. Rheol.* **41** 197
[13] Rueb C J and Zukoski C F 1998 *J. Rheol.* **42** 1451
[14] Bibette J, Mason T G, Gang H and Weitz D A 1992 *Phys. Rev. Lett.* **69** 981
[15] Meller A, Gisler T, Weitz D A and Stavans J 1999 *Langmuir* **15** 1918
[16] Piazza R and di Pietro G 1994 *Europhys. Lett.* **28** 445
[17] Kline S R and Kaler E W 1996 *Langmuir* **12** 2402
[18] George A and Wilson W W 1994 *Acta Crystallogr.* D **50** 361
[19] Rosenbaum D, Zamora P C and Zukoski C F 1995 *Phys. Rev. Lett.* **76** 150
[20] Muschol M and Rosenberger F 1997 *J. Chem. Phys.* **107** 1953
[21] Velev O D, Kaler E W and Lenhoff A M 1998 *Biophys. J.* **75** 2682
[22] Gast A P, Hall C K and Russel W B 1983 *J. Colloid Interface Sci.* **96** 251
[23] Gast A P, Russel W B and Hall C K 1986 *J. Colloid Interface Sci.* **109** 161
[24] Canessa E, Grimson M J and Silbert M 1989 *Mol. Phys.* **67** 1153
[25] Lekkerkerker H N W, Poon W C K, Pusey P N, Stroobants A and Warren P B 1992 *Europhys. Lett.* **20** 559
[26] Tejero C F, Daanoun A, Lekkerkerker H N W and Baus M 1994 *Phys. Rev. Lett.* **73** 752

[27] Hagen M H J and Frenkel D 1994 *J. Chem. Phys.* **101** 4093
[28] Lekkerkerker H N W, Dhont J K G, Verduin H, Smits C and van Duijneveldt J S 1995 *Physica* A **213** 18
[29] Poon W C K, Pirie A D, Haw M D and Pusey P N 1997 *Physica* A **235** 110
[30] Bergenholtz J and Fuchs M 1999 *Phys. Rev.* E **59** 5706
[31] Götze W 1991 *Liquids, Freezing and Glass Transition* ed J-P Hansen, D Levesque and J Zinn-Justin (Amsterdam: North-Holland)
[32] Götze W and Sjögren L 1991 *Phys. Rev.* A **43** 5442
[33] Götze W and Sjögren L 1992 *Rep. Prog. Phys.* **55** 241
[34] Doliwa B and Heuer A 1998 *Phys. Rev. Lett.* **80** 4915
[35] Verduin H, de Gans B J and Dhont J K G 1996 *Langmuir* **12** 2947
[36] Poon W C K, Starrs L, Meeker S P, Moussaid A, Evans R M L, Pusey P N and Robins M M 1999 *Faraday Discuss.* **112** 143
[37] Pusey P N and van Megen W 1987 *Phys. Rev. Lett.* **59** 2083
[38] van Megen W and Pusey P N 1991 *Phys. Rev.* A **43** 5429
[39] van Megen W and Underwood S M 1994 *Phys. Rev.* E **49** 4206
[40] van Megen W 1995 *Transport Theory Stat. Phys.* **24** 1017
[41] Götze W and Sjögren L 1995 *J. Math. Anal. Appl.* **195** 230
[42] Waisman E 1973 *Mol. Phys.* **25** 45
[43] Hoye J S and Blum L 1977 *J. Stat. Phys.* **16** 399
[44] Cummings P T and Smith E R 1979 *Chem. Phys.* **42** 241
[45] Kawasaki K 1976 *Phase Transitions and Critical Phenomena* ed C Domb and M S Green (New York: Academic)
[46] Fabbian L, Götze W, Sciortino F, Tartaglia P and Thiery F 1999 *Phys. Rev.* E **59** R1347
Fabbian L, Götze W, Sciortino F, Tartaglia P and Thiery F 1999 *Phys. Rev.* E **60** 2430
[47] Krall A H and Weitz D A 1998 *Phys. Rev. Lett.* **80** 778